

# Hollow Fiber Hemodialysis Imprinted Membrane Based on Eugenol for Human Blood Filter

Muhammad Cholid Djunaidi<sup>1\*</sup>, Nesti Dwi Maharani<sup>1</sup>, Pardoyo Pardoyo<sup>1</sup>, and Yanuardi Raharjo<sup>2</sup>

<sup>1</sup>Department of Chemistry, Faculty of Science and Mathematics, Diponegoro University, Jl. Prof. Soedharto SH, Tembalang, Semarang 50275, Indonesia

<sup>2</sup>Department of Chemistry, Faculty of Science and Technology, Universitas Airlangga, Campus C, Mulyorejo, Surabaya 60115, Indonesia

\* **Corresponding author:**

email: choliddjunaidi@lecturer.undip.ac.id

Received: March 14, 2023

Accepted: June 1, 2024

DOI: 10.22146/ijc.83065

**Abstract:** Kidney failure is a kidney function disorder that occurs in more than 90.00% of people in the world, especially in developing countries. In 2013, around 12.50% of the 25 million population experienced kidney failure and 78.00% had to undergo dialysis for life. In this research, a hemodialysis method was developed, namely molecularly imprinted membrane (MIM), which has high selectivity for urea molecules with high binding capacity using a membrane in the form of hollow fiber. Variations in research use urea transport concentrations such as 50, 200, and 300 ppm. The analysis using UV-vis spectrophotometry on HFHIM with a solution mixture of 50 ppm showed that the receiving phase by the membrane was 70.48% urea, 12.97% creatinine, and 9.42% vitamin B<sub>12</sub>. Meanwhile, the feed phase is 28.25% urea, 85.41% creatinine and 88.64% vitamin B<sub>12</sub>. When using HFHNIM, the receiving phase is urea 44.78%, creatinine 58.51%, and vitamin B<sub>12</sub> 31.00%. Meanwhile, the feed phase is 54.55% urea, 40.57% creatinine, 68.29% vitamin B<sub>12</sub>. The selectivity of HFHIM for urea is better than creatinine and vitamin B<sub>12</sub> compared to HFHNIM, in the order of selectivity urea > creatinine > vitamin B<sub>12</sub>.

**Keywords:** polyeugenol; imprinted; hollow fiber; hemodialysis

## ■ INTRODUCTION

Kidney failure is a disease often experienced by some parts of the world community, especially developing countries, where the kidneys experience a permanent decline in function of more than 90.0% [1]. The kidneys experience a decrease in the ability to filter sodium, potassium, urea, and creatinine in the blood [2]. Based on data from the Indonesian Nephrology Association, around 12.5% of the 25 million population experienced kidney failure in 2013 [3]. About 78.0% have to be under dialysis for the rest of their lives. Factors that cause kidney failure are too often consuming preservative drinks, drinking tea and coffee, smoking, energy supplement drinks, age, hypertension, and diabetes [4]. Several methods that have been carried out to overcome this problem while preserving the patient's life, one of which is kidney transplantation and hemodialysis by separating 66–75%

of urea in the blood into a series of dialyzer devices (artificial kidney) using a semi-permeable membrane until kidney function recovers [4-5]. The membrane used must be strong, porous, not leaky, selective, using a simple method, cheap and, of course, not rejected by the blood (hemocompatible) and able to separate urea and creatinine in the blood [6]. The threshold value for urea in the body is around 15–40 mg/dL while creatinine is around 0.7–1.5 mg/dL. If it exceeds the limit, it will become toxic. This therapy is usually done 2 or 3 times a week for 4–5 h. However, this therapy is very expensive, takes a long time, and the tools are few, while the patients are many, so it is necessary to develop better analytical methods, have high sensitivity and selectivity, as well as better separation and preconcentration technology [7].

One of the developments of the hemodialysis method is the molecularly imprinted membrane (MIM)

method which has high selectivity because it involves molecular imprints. The MIM is a method or technique for making templated membranes, so they are selective for target molecules with high binding capacity and excellent permeability [8-15]. Djunaedi et al. [16] conducted research using eugenol derivative as a functional polymer with polyethylene glycol (PEG) for the synthesis of MIM glucose for selective transport of glucose. In 2020, Djunaedi et al. [17] conducted further research on membrane selectivity from eugenol derivative to determine the effect of adsorption on Au(III) metals in polysulfone solutions in NMP solvents. In addition, Djunaedi et al. [18] have conducted research using eugenol derivative as a functional polymer with PEG 6000 in NMP to get the best results of MIM for the selective transport of urea. From the various problems that have been studied regarding the matters above, it is necessary to synthesize hollow fiber hemodialysis imprinted membrane (HFHIM) with a polyeugenol component as a functional polymer with polysulfone and PEG 6000 which is expected to be able to adsorb urea and creatinine properly. To determine the adsorption selectivity, a comparison was made with performance HFHIM based on eugenol and the selectivity of urea adsorption on other components such as creatinine and vitamin B<sub>12</sub>.

## ■ EXPERIMENTAL SECTION

### Materials

Materials used in this study are eugenol (Sigma Aldrich), BF<sub>3</sub>O(C<sub>2</sub>H<sub>5</sub>)<sub>2</sub> (Sigma Aldrich), anhydrous Na<sub>2</sub>SO<sub>4</sub> (Merck), Na<sub>2</sub>HPO<sub>4</sub> (Merck), NaH<sub>2</sub>PO<sub>4</sub> (Merck), HCl (Merck), NaOH (Merck), methanol (Merck), chloroform (Merck), ethanol (Merck), urea (Merck), creatinine (Merck), vitamin B<sub>12</sub> (Merck), 4-(dimethylamino)benzaldehyde (Merck), picric acid (Sigma Aldrich), aquabides (Brataco Chem), polysulfone (PSF, Sigma Aldrich), *N*-methyl-2-pyrrolidone (NMP, Merck), and PEG 6000 (Merck).

### Instrumentation

The instrumental used in this research were analytical balance (Mettler-200 and Ohaus), stirrer, pH meter (Trans Instrument), casting machine, UV-vis spectrophotometer

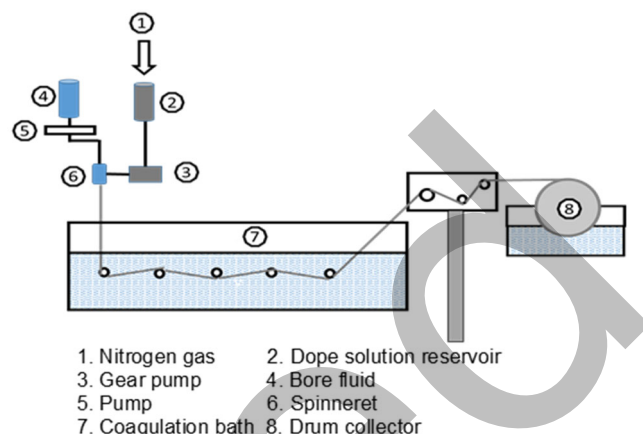


**Fig 1.** Hollow fiber printing equipment range [13]

(LW-V-200-RS), FTIR (Shimadzu Prestige 21), ASTM, SEM-EDX (JEOL JSM 6510 LA), thickness meter (Digilife), Ubbelohde viscosimeter, TGA/DTA (Exstar SII 7300), HT-2402 computer universal testing machines, reflux apparatus, T3 pots, digital caliper, ovens (Faithful FCD-300 Serials), peristaltic pump and hose, and an instrument for making hollow fiber (Fig. 1), pestle and mortar.

### Procedure

#### **MIM-urea synthesis**

**Polyeugenol (PE) synthesis.** An amount of 5 g of eugenol was put in a three-neck flask and then 1 mL of BF<sub>3</sub>O(C<sub>2</sub>H<sub>5</sub>)<sub>2</sub> was added. The mixture was stirred and 0.25 mL of BF<sub>3</sub>O(C<sub>2</sub>H<sub>5</sub>)<sub>2</sub> was added every 1 h. After 4 h, the polymerization was stopped by adding 1 mL of methanol. The gel formed was dissolved with chloroform and washed with distilled water until the pH was neutral. The solution is dried by adding anhydrous Na<sub>2</sub>SO<sub>4</sub> and evaporated at room temperature. The precipitate formed was then dried, weighed, and analyzed by FTIR.

#### **MIM-urea contact**

PE synthesized as much as 1 g was contacted with a urea concentration of 1000 ppm with aquabidest in a 25 mL volumetric flask. This aims to include a molecule (template) of urea. Then it was stirred for 24 h and then filtered and dried to form PE-urea.

#### **HFHIM based on eugenol**

PE-urea was added to polysulfone and PEG 6000 in a 1:4:1 weight ratio with 0.25 mL of AIBN catalyst

dissolved in 12 mL of NMP solvent, stirred and refluxed for 10 h at 90 °C. After being homogeneous or united, the dope membrane is printed using the phase inversion method on a membrane printing device. A coagulant bath filled with water that is at room temperature is placed under the spinneret as far as 30 cm above the water surface. The dope solution is put in tube 1 (dope tube). In tube 2, distilled water is flowed by adjusting the flowmeter. Tube 1, which contains a dope solution, is connected to the compressor using a hose. Then, the water and compressor are opened to start the formation of hollow fiber membranes. After passing through the spinneret, the dope solution enters the coagulant bath to form a dense hollow fiber. The dense hollow fiber membrane is washed with running water to remove residual solvent. After that, it was put in a bath containing sodium azide solution until the hollow fiber was characterized. Synthesis HFHNIM (control) was also performed but the synthesized PE was not contacted with 1000 ppm urea.

#### **Transport urea, creatinine and vitamin B<sub>12</sub> HFHIM and HFHNIM**

Membrane transport is performed on HFHIM and HFHNIM as follows. First, HFHIM and HFHNIM were used to transport urea solution with various concentrations of 50, 200, and 350 ppm using a series of transport devices. This transport was carried out by taking 2 mL of the sample every 1 h for 6 h, complexed (DAB) and measured by a UV-vis spectrophotometer at a wavelength of 430 nm. Second, HFHIM and HFHNIM were used to transport 50 ppm creatinine solution using a series of transport devices. This transport was carried out by taking 2 mL of sample every 1 h for 6 h, complexed (picric acid) and measured using a UV-vis spectrophotometer at 486 nm. Third, HFHIM and HFHNIM were used to transport of 50 ppm vitamin B<sub>12</sub> solution using a series of transport devices. This transport was carried out by taking 2 mL of sample every 1 h for 6 h and was measured by a UV-vis spectrophotometer at 361 nm.

#### **Characterization**

**Flux Test.** A total of 10 strands of HFHIM and HFHNIM were strung (Fig. 2), which were flowed with a peristaltic pump using various solutions, i.e., distilled water, 50 ppm

urea, 50 ppm creatinine and 50 ppm vitamin B<sub>12</sub> as much as 1 L in 1 bar pressure for 1 h. The flux value (J) is calculated using Eq. (1):

$$J = \frac{V}{A \cdot t} \quad (1)$$

where, V is permeate volume (L), A is surface area of the membrane (m<sup>2</sup>), and t is time (h)

**Biodegradable test.** The initial weight of the membrane was measured, then placed in the fertilizer or soil and observed every week to find out the final weight produced.

**Membrane Porosity Test.** The membrane was soaked with 10 mL of aquadamine in a petri dish for 24 h at room temperature, dried and weighed so that the value of W<sub>1</sub> (g) is obtained. Furthermore, the membrane was dried in an oven at 100 °C for 6 h, then cooled and weighed again so that the value of W<sub>2</sub> (g) was obtained as the dry weight of the membrane.

**Water uptake test.** The membrane was weighed to obtain the membrane's initial weight, then immersed in 10 mL of aquadamine for 6 h and weighed again after immersion. All of the tests were repeated 3 times.

## ■ RESULTS AND DISCUSSION

### PE Synthesis

PE can be synthesized from eugenol because it has 3 functional groups, namely allyl groups, hydroxy groups and methoxy groups. This allyl (propenyl) group

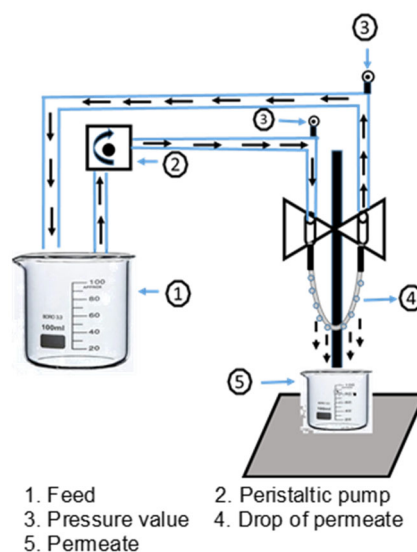


Fig 2. Hollow fiber flux test equipment series [13]

can be polymerized cationically into a  $\beta$ -styrene group derivative. Polymerization usually uses Friedel-Craft catalysts such as  $\text{AlCl}_3$ ,  $\text{AlBr}_3$ ,  $\text{BF}_3\text{O}(\text{C}_2\text{H}_5)_2$ ,  $\text{TiCl}_4$ ,  $\text{H}_2\text{SO}_4$ , and other strong acids [15-16]. Polymerization occurs through 3 stages (Fig. 3).

First, through the initiation stage, with the addition of the  $\text{BF}_3\text{O}(\text{C}_2\text{H}_5)_2$  catalyst, it functions as an initiator in the cationic process (a compound that accepts electrons). The allyl group of eugenol undergoes a gradual addition reaction, which is often called a cationic addition process [16]. The propagation occurs in the formation of covalent bonds in the cation chain of the eugenol monomer, resulting in a long monomer chain. The termination stage, with the addition of methanol, functions to stop the polymerization process so that the carbonium ion bonds with its partner anion ( $\text{CH}_3\text{O}$  group) and the end of the PE polymer is a methoxy group [16-17]. The PE produced was in the form of an orange powder with a yield of

98.85%. The molecular weight of eugenol is 164.20, so the degree of polymerization of PE synthesis using the  $\text{BF}_3\text{O}(\text{C}_2\text{H}_5)_2$  catalyst produces a relative molecular mass of 6323.65 g/mol and a degree of repeatability of 38.51 ( $\sim 38$  monomers).

Fig. 4 shows the results of the FTIR analysis of PE. It appears that there is no spectral formation of the allyl group ( $\text{C}=\text{C}$ ) at  $1643.351\text{ cm}^{-1}$  and vinyl groups ( $\text{C}=\text{CH}_2$ ) at  $995.269$  and  $910.401\text{ cm}^{-1}$ . So, it can be concluded that there has been a polymerization reaction. The group undergoes an addition reaction upon polymerization [16], and the polymerization reaction can be an addition reaction. Thus, the process of making PE was successfully carried out.

#### Contact with Urea Solution

The urea solution used for contacting was at a pH of 7.4 (same as blood pH) with a concentration of around

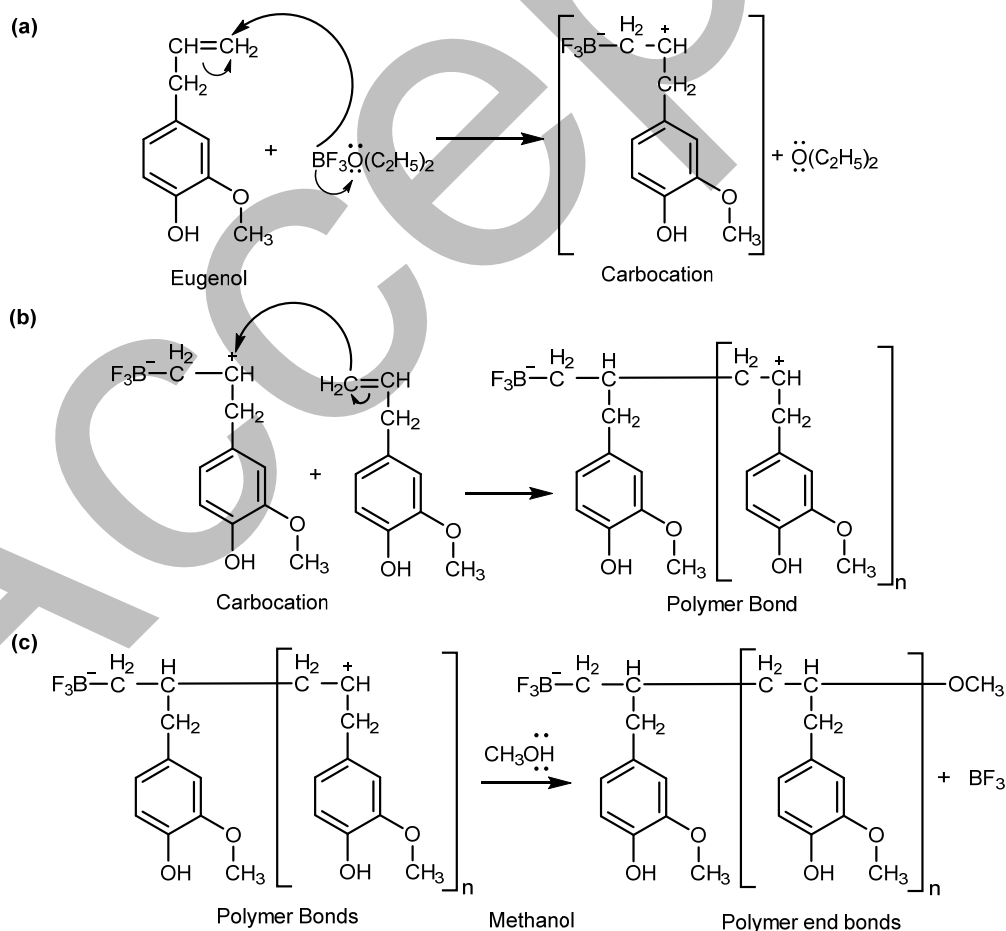


Fig 3. Polymerization mechanism of eugenol: (a) initiation, (b) propagation, and (c) termination stages [16]

1000 ppm. Table 1 shows that the contact urea on the polymer reaches 74.38% with a concentration of 720.27 ppm. This is due to the non-covalent interactions that occur repeatedly in the printing process with PE because the interactions that occur have relatively weak bonds, such as hydrogen bonds. The possible reactions are shown in Fig. 5 [18].

The FTIR results show a comparative analysis as shown in Fig. S1, S2, and 6. From the results of the analysis of Fig. S1 using the Fityk software, it shows that there are 5 absorption peaks below the actual peak. Five absorption peaks were found at 1585.42, 1600.86 (C=C aromatic), 1653.25 (N-H) [16], 1677.26, and 1712.39  $\text{cm}^{-1}$  (C=O of amides).

Fig. S2 shows that there are 4 absorption peaks below the actual peak. Four absorption peaks were found at 1575.54, 1603.82 (C=C aromatic), 1642.48, and 1673.34  $\text{cm}^{-1}$  (C=C alkene). Thus, peaks 3, 4, and 5 (in Fig. S1) in the uptake analysis of urea-contacted PE. So, it can be concluded that the PE has been successfully templated with urea. Fig. 6 shows the results of the FTIR analysis that there is absorption of OH groups at 3415  $\text{cm}^{-1}$ , C=C aromatic at 1582  $\text{cm}^{-1}$ , C- $sp_3$  at 1488.25  $\text{cm}^{-1}$ , S=O at 1243.25  $\text{cm}^{-1}$ , C-SO<sub>2</sub>-C at 1104  $\text{cm}^{-1}$ , and C-O at 1151.25  $\text{cm}^{-1}$  (at magnification) [16]. The OH group in PE-urea showed an increase in intensity compared to PE, but when it was used to bind to polysulfone and PEG 6000, the intensity of the OH group decreased greatly in HFHIM and HFHNIM. This is because crosslinking occurs using the OH group of PEG while the CO group increases. These results are in accordance with previous researchers [17]. The cross-linking reaction maintains the optimal alignment of the functional groups that bind to the template molecule. The conjugate structure is locked in a three-dimensional network of polymers such as PE-urea cross-links, polysulfone and PEG 6000, as shown in Fig. 7.

Fig. 8 shows the results of TGA analysis using the thermal analysis method on variations of HFHIM and HFHNIM, which aims to determine the level of membrane stability that varies with the influence of temperature. HFHIM T<sub>1-5%</sub> mass decrease occurs in the temperature range 141.17–365.33 °C and HFHNIM T<sub>1-5%</sub>

mass decrease occurs in 98.58–316.61 °C due to the escape of water molecules. HFHIM mass decrease T<sub>6-98%</sub> occurs in 378.4–762.98 °C and HFHNIM mass decrease T<sub>6-98%</sub> occurs in 337.6–709.22 °C due to depolymerization

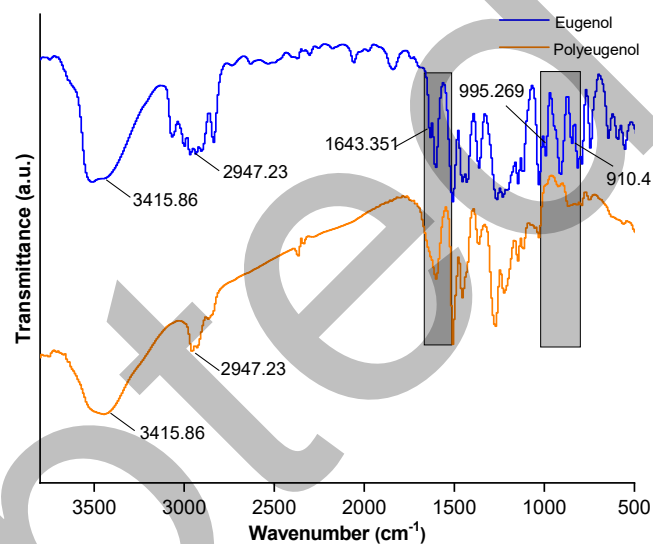


Fig 4. FTIR comparison results of eugenol and PE

Table 1. PE-urea contact result data

Synthesis Pe-urea	Before contact	After contact	Adsorbed concentration
Urea (ppm)	968.32	248.05	720.27

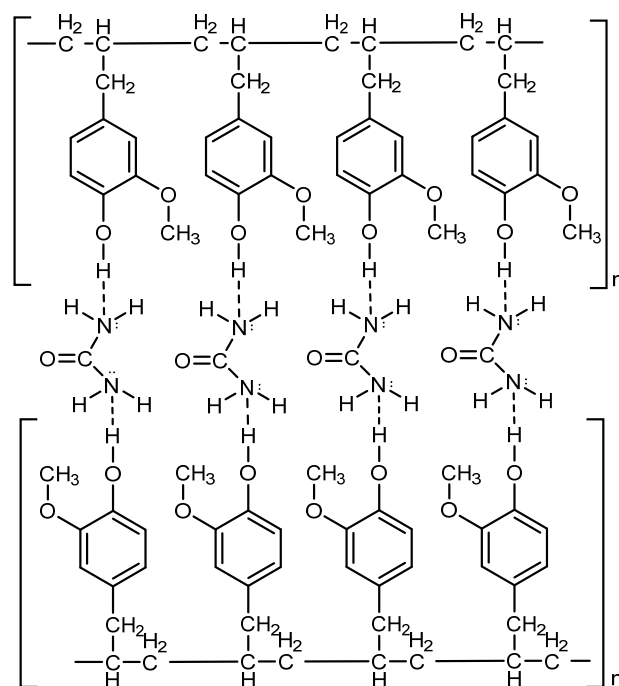


Fig 5. Estimated interaction between PE and urea



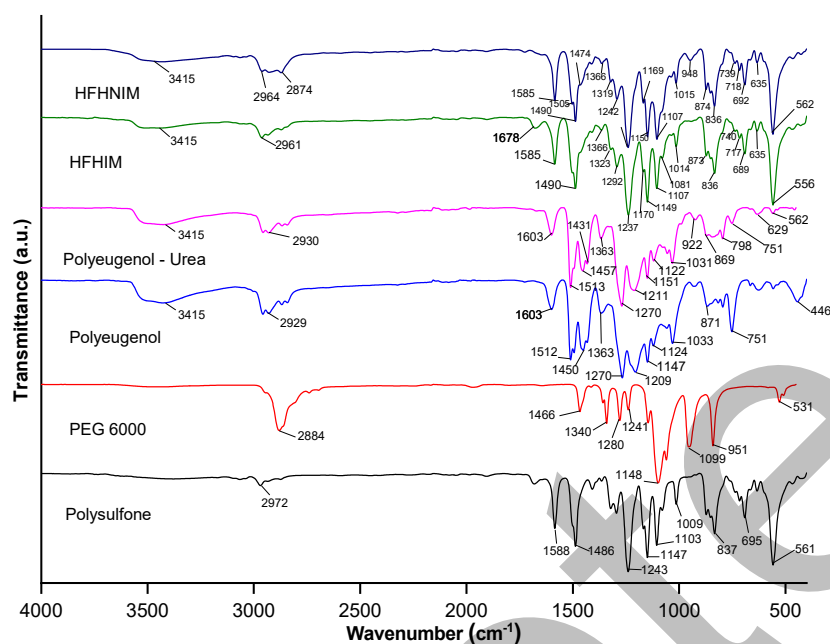


Fig 6. FTIR results comparison between HFHIM and HFHNIM

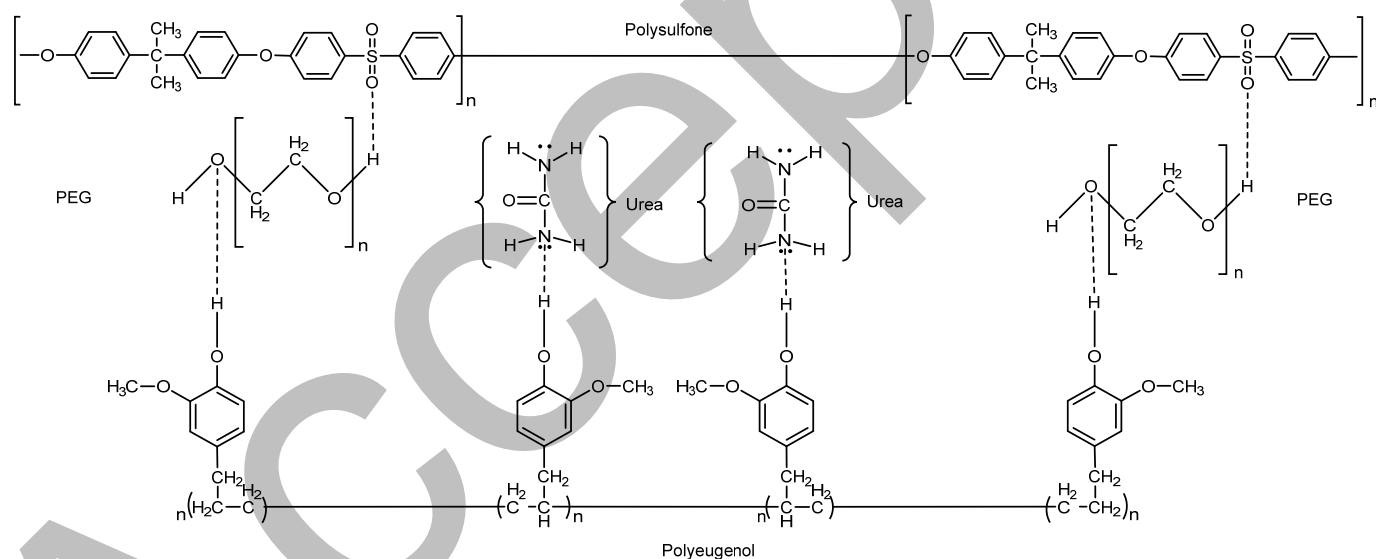


Fig 7. Estimation interaction between PE and urea

of the benzene ring and the process of imprinting the molecule produces many cavities in the membrane, and the chemical stability increases. Chemical stability is influenced by intermolecular bonds, which require more energy for degradation [19-20]. We can conclude that with the addition of a template urea has a lower degradation temperature, which has the potential to disrupt polymer chains, especially hydrogen bonds, so

that they tend to be unstable and more brittle [21-22].

SEM results show the effect of imprinted urea on membrane morphology using 5000× magnification. The cross-section of the membrane uses a magnification of 60×. Fig. 9 and Table 2 show the results of surface morphology and cross-section using SEM. The morphology of the HFHNIM membrane has pores that are not uniform in size compared to HFHIM in the form

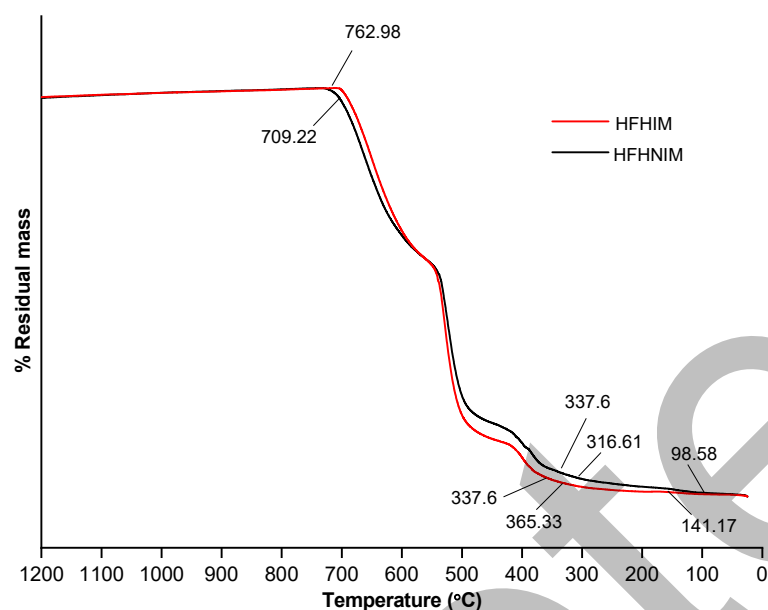


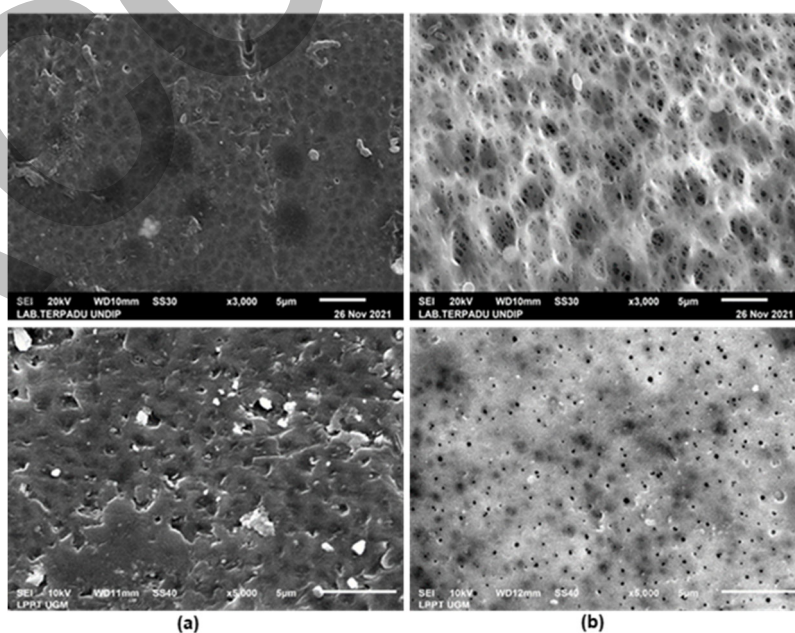
Fig 8. TGA comparison results between HFHIM and HFHNIM

of composite asymmetry. The cross-section of the HFHIM membrane forms a finger-like macrovoid compared to the HFHNIM image [7,18]. This is because when the hollow fiber membrane, after being printed, is then immersed in a coagulation bath containing aquabidest the membrane will precipitate and the formation of membrane pores occurs due to the weak solubility of the three materials in water, causing the

exchange of NMP solvents with water much more quickly to form macrovoid finger like.

Table 2. Comparison of pore size between HFHIM and HFHNIM membranes with Image J

	HFHIM	HFHNIM
Counted number of pores	259687	173395
Total areas	159.011	78.608
% Area	36.314	14.483



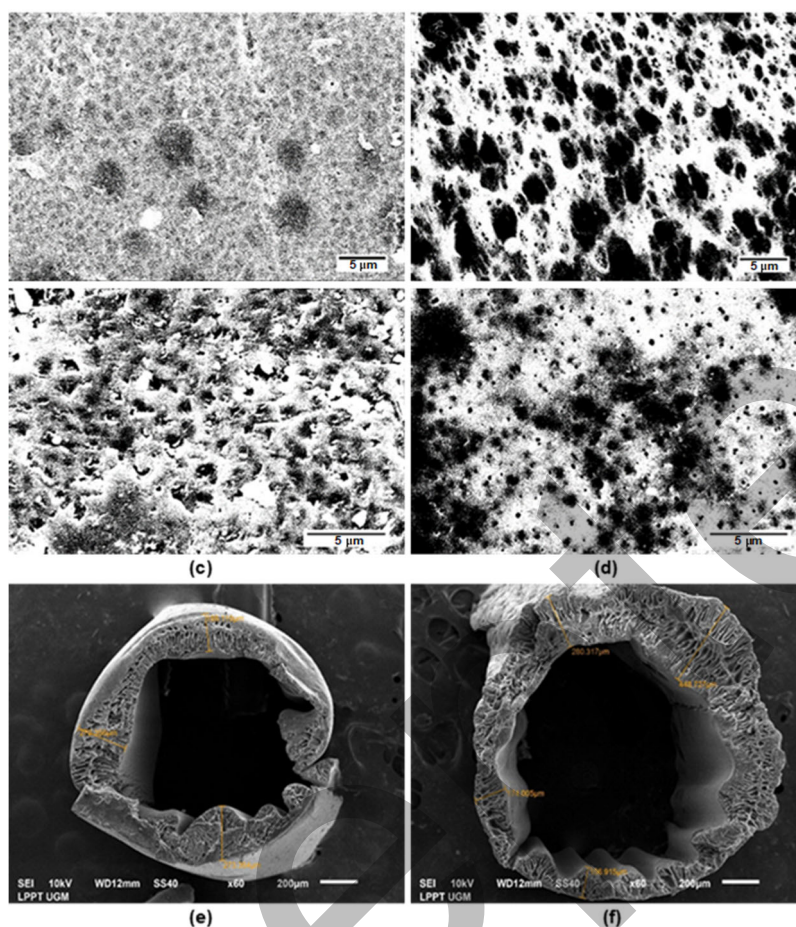


**Fig 9.** Membrane SEM results of (a) HFHNIM, (b) HFHIM, (c) HFHNIM with Image J, (d) HFHIM with Image J, the cross section of (e) HFHNIM, and (f) HFHIM

### Flux Test Using HFHIM and HFHNIM with Urea Creatinine and Vitamin B<sub>12</sub> Solution

Fig. 10 shows the results of the flux test due to the influence of urea molding, that is, the result of flux measurements on HFHIM and HFHNIM, which aims to determine the size of the pores in the membrane using various types of solutions that have different molecular weights such as water, urea, creatinine, and vitamin B<sub>12</sub>. If the higher the value of the membrane flux describes the pores in the membrane (macrovoid) the solution can pass through [23-24]. The HFHIM has a water flux value of 531.10 L/m<sup>2</sup> h, urea of 517.73 L/m<sup>2</sup> h, creatinine of 101.89 L/m<sup>2</sup> h, and vitamin B<sub>12</sub> of 47.76 L/m<sup>2</sup> h. HFHNIM has a percentage of water flux value of 519.64 L/m<sup>2</sup> h, urea of 493.53 L/m<sup>2</sup> h, creatinine of 493.53 L/m<sup>2</sup> h, and vitamin B<sub>12</sub> of 560.40 L/m<sup>2</sup> h. This is due to the presence of a template molecule of urea of around 60 g/mol in the

membrane so that the target molecule only recognizes urea and water (as solvents) compared to creatinine and vitamin B<sub>12</sub>. The size of the creatinine and vitamin B<sub>12</sub> molecules is larger than urea, around 113.00 g/mol (creatinine) and 8.50 Å or 1350.00 g/mol (vitamin B<sub>12</sub>) [13,18].

### Porosity Test on HFHIM and HFHNIM

Fig. 11 shows the results of porosity measurements on HFHIM and HFHNIM, which aim to determine the number of interactions that occur between the membrane and water molecules (how much the membrane can adsorb), the higher the porosity of the membrane, and the number of empty space (macrovoid) in the membrane [25-26].

From the data, HFHIM has a bigger percentage (89.04%) than HFHNIM (68.24%) due to the addition of



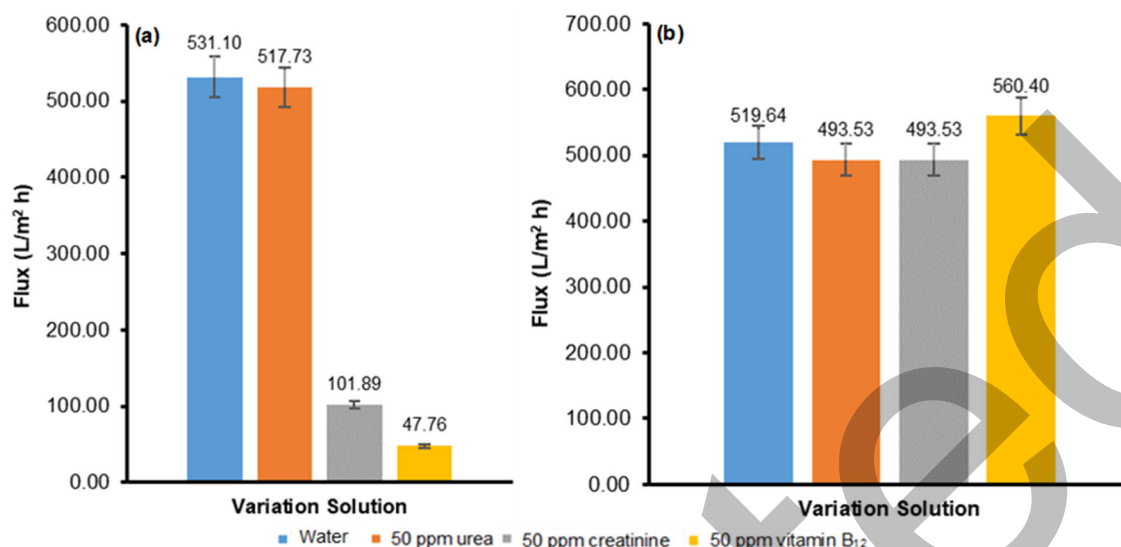


Fig 10. Membrane flux of (a) HFHIM and (b) HFHNIM

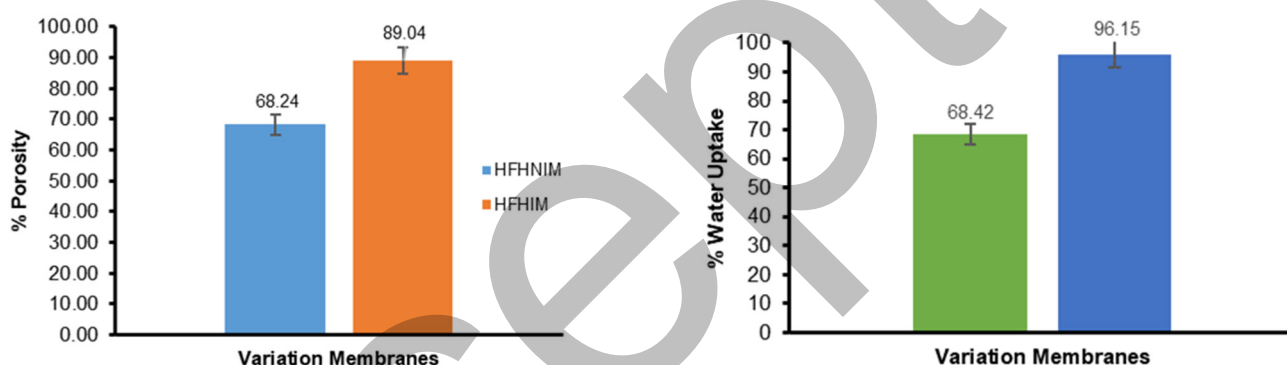


Fig 11. Membrane porosity of (a) HFHIM and (b) HFHNIM

Fig 12. Membrane water absorption of (a) HFHIM and (b) HFHNIM

a urea template, which has a hydrophilic OH group so that more water molecules are absorbed into the pores of the membrane because it can form physical interactions such as intermolecular hydrogen bonds between the functional groups of membrane constituent compounds (OH) and water that is able to pass through the pores of the membrane [27].

#### Water Absorption Test on HFHIM and HFHNIM

Fig. 12 shows the results of measuring water absorption on HFHIM and HFHNIM, which aims to determine the ability of the membrane to absorb water (the number of empty membrane cavities that interact with water) the higher the water absorption of the membrane, and the number empty space (macrovoid) in the membrane [28-29]. HFHIM has a bigger water absorption

percentage (96.50%) than HFHNIM (68.42%) due to the addition of a urea template, so that increased water absorption [13].

#### Biodegradable Test on HFHIM and HFHNIM

Fig. 13 shows the results of the biodegradable test on HFHIM and HFHNIM, which aim to determine how long the membrane constituent material can be completely degraded. The faster the membrane mass decreases, the better the membrane material decomposes quickly and is safe for the environment [30]. The percentage value of biodegradable in HFHIM (18%) is smaller than HFHNIM (23.4%) due to the addition of a urea template, making it easier for microorganisms to decompose [31]. The increase in the biodegradable test is directly proportional to the results of

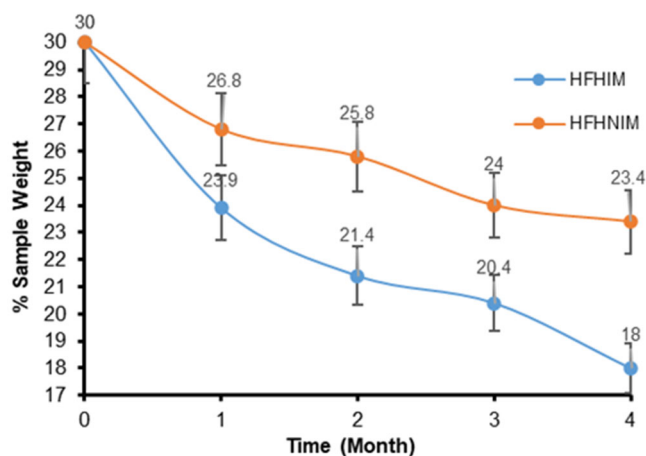


Fig 13. Biodegradability of (a) HFHIM and (b) HFHNIM

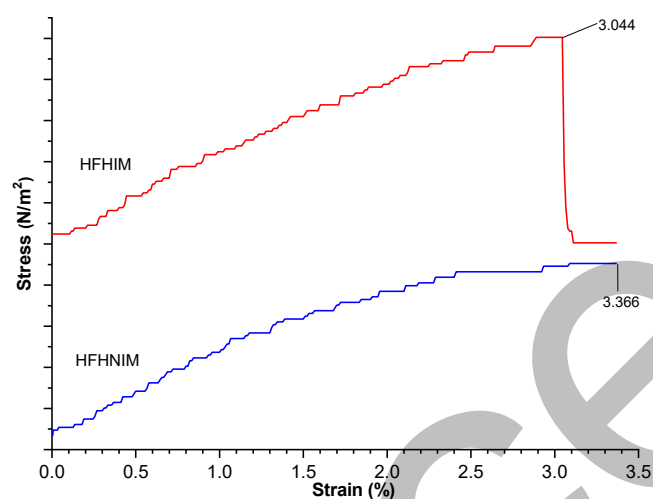


Fig 14. Membrane tensile test of (a) HFHIM and (b) HFHNIM

Table 3. Comparison of Young's modulus values between HFHIM and HFHNIM membranes

Membranes variation	Strains (%)	Stress (N/M <sup>2</sup> )	Young's Modulus (N/M <sup>2</sup> )
HFHIM	3.044	2005	0.6587
HFHNIM	3.366	0.905	0.2689

the porosity, water absorption and flux test.

### Tensile Test on HFHIM and HFHNIM

Fig. 14 and Table 3 show the results of tensile test measurements on HFHIM and HFHNIM, which aim to determine the strength of the membrane constituent material (mechanical properties of the membrane), which can be seen from the large Young's modulus value. The

greater the Young's modulus value, the better the membrane material decomposes quickly and is safe for the environment. The Young's modulus value of HFHNIM is decreased ( $0.2689 \text{ N/M}^2$ ), compared to the HFHIM value ( $0.6587 \text{ N/M}^2$ ) due to the addition of a urea template with hydrophilic OH groups so that the strength needed to destroy the membrane. The increase in the tensile test is directly proportional to the results of the biodegradable test [30].

### Urea Transport with Urea Concentration Variations using HFHIM and HFHNIM

Urea transport uses 3 concentration variations (50, 200, and 350 ppm) which aims to determine the optimum concentration of transport in HFHIM and HFHNIM. Fig. 15 shows the results of urea transport with a concentration variation of 50 ppm, that the percentage of urea transport in HFHIM is 70% in the receiving phase and 28% remaining in the feed phase. Whereas in HFHNIM, it is 45% in the receiving phase and the remaining in the feed phase is 55%. At a concentration variation of 200 ppm, the percentage of urea transport in HFHIM was 69% in the receiving phase and 30% remaining in the feed phase. Whereas in HFHNIM it is 35% in the receiving phase and the remaining in the feed phase is 63%. Meanwhile, at a concentration variation of 350 ppm, the percentage of urea transport in HFHIM was 72% in the receiving phase and 26% remained in the feed phase. Whereas in HFHNIM, it is 37% in the receiving phase and the remaining in the feed phase is 62%. Thus, the transport of HFHIM is much larger than that of HFHNIM.

### Creatinine Transport Using HFHIM and HFHNIM

Creatinine transport was carried out by comparing HFHIM and HFHNIM membranes. Fig. 16(a) shows the results of 50 ppm creatinine transport in HFHIM, the percentage of transport is 13% in the receiving phase and 85% in the feed phase. Meanwhile, in HFHNIM the percentage of transport in the receiving phase is 59 and 41% is in the feed phase. Based on data, optimal results are obtained using HFHIM due to the presence of a printed molecule (template) urea in the membrane so that the target molecule only recognizes urea compared

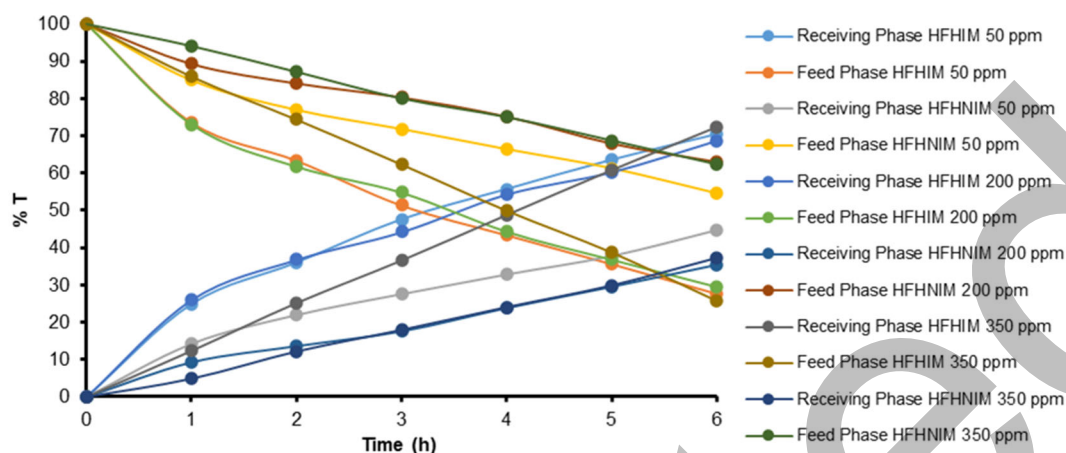


Fig 15. Percentage of urea transport results with concentration variations in HFHIM and HFHNIM

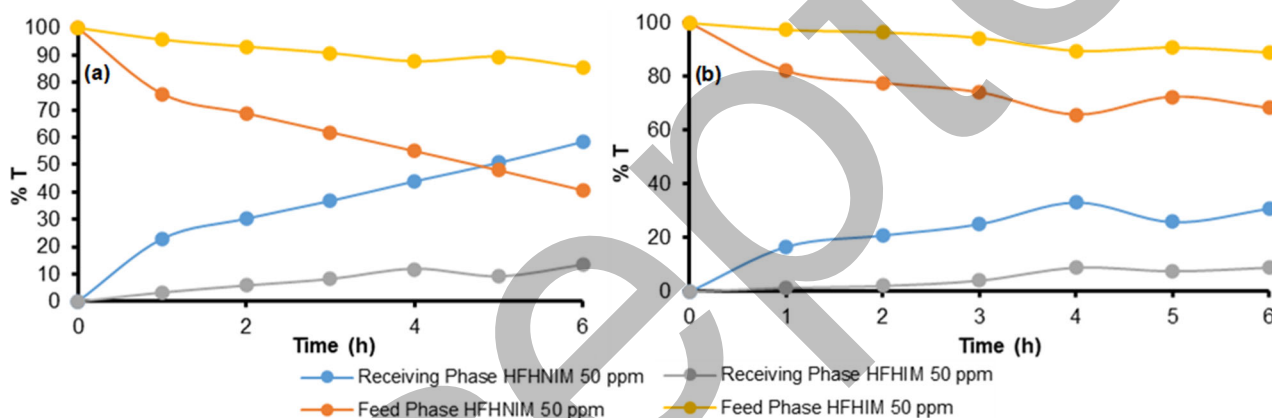


Fig 16. Percentage of (a) creatinine and (b) vitamin B<sub>12</sub> transport in HFHIM and HFHNIM

to creatinine, and the size of the creatinine molecule (113.00 g/mol) [32] is larger than urea (60.00 g/mol) [18] so HFHIM is more selective than HFHNIM.

#### Transport Vitamin B<sub>12</sub> Using HFHIM and HFHNIM

Vitamin B<sub>12</sub> transport is carried out by comparing HFHIM and HFHNIM membranes. This compound was chosen because it is the main compound in the blood, besides urea and others. Fig. 16(b) shows the results of the transport of 50 ppm vitamin B<sub>12</sub>. In HFHNIM the optimal percentage results were 31% in the receiving phase and 68% in the feed phase. Meanwhile, HFHIM obtained optimal percentage results of 9% in the receiving phase and 89% in the feed phase. So, with an imprint on the percentage results, results that should be optimal using HFHIM are obtained. This is due to the presence of a template molecule of urea in the membrane so that the

target molecule only recognizes urea compared to vitamin B<sub>12</sub>, which is larger than urea [33]. Determining the selectivity of the membrane on vitamin B<sub>12</sub> is an indicator for hemodialysis because of its binding to plasma proteins, but the indicators of urea and creatinine are much more important [14].

#### Mixed Transport Using HFHIM and HFHNIM

Measuring the levels of urea, creatinine, and vitamin B<sub>12</sub> in mixed solutions aims to determine HFHIM ability to analyze urea in samples of mixed solutions. Fig. 17 shows the results of transporting a mixed solution of 50 ppm each using HFHIM, the optimal percentage of urea was 70.48% in the receiving phase and 28.25% in the feed phase. Creatinine was 12.97% in the receiving phase and 85.41% in the feed phase and vitamin B<sub>12</sub> was 9.42% in the receiving phase

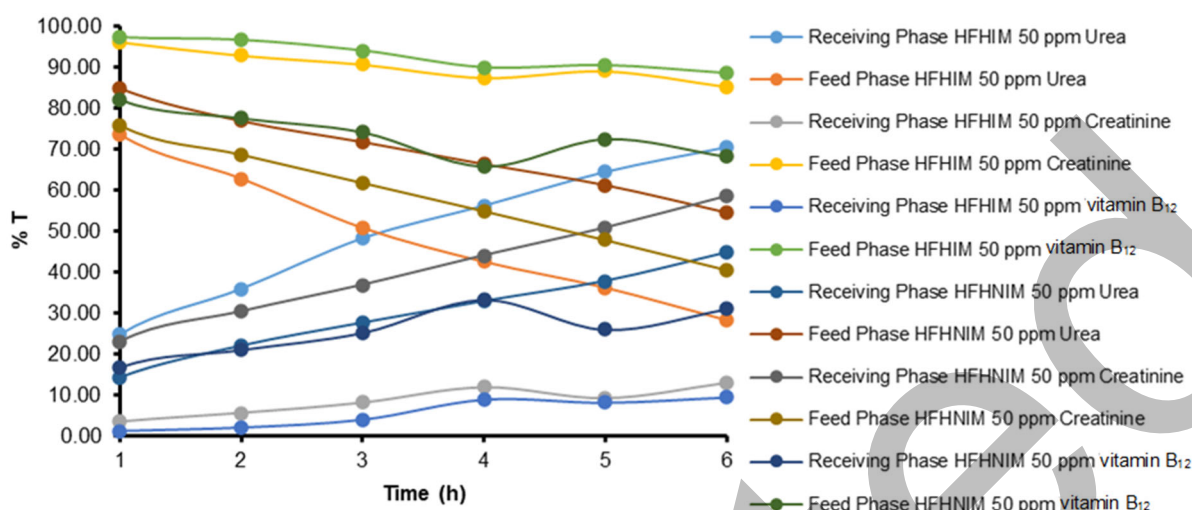


Fig 17. Mixed solution transport percentage in HFHIM and HFHNIM

and 88.64% in the feed phase. On HFHNIM, the optimal percentage of urea was 44.78% in the receiving phase and 54.55% in the feed phase, creatinine was 58.51% in the receiving phase and 40.57% in the feed phase, and vitamin B<sub>12</sub> 31% in the receiving phase and 68.29% in the feed phase. This is due to the presence of a printed molecule (template) of urea in the membrane so that the target molecule will be better recognized in transporting urea. The selectivity of urea for creatinine and vitamin B<sub>12</sub> shows that HFHIM is better at transporting urea than creatinine and vitamin B<sub>12</sub> so the order of selectivity is urea > creatinine > vitamin B<sub>12</sub>.

#### HFHIM and HFHNIM Selectivity for Urea, Creatinine and Vitamin B<sub>12</sub>

##### HFHIM and HFHNIM selectivity for urea vs. creatinine

The membrane selectivity test was carried out by comparing HFHIM and HFHNIM membranes in transporting urea and creatinine at 50 ppm each in separate solutions. HFHIM will be more optimal in transporting urea than HFHNIM due to the presence of a printed molecule (template) of urea in the membrane so that the target molecule will be better recognized in transporting urea.

Fig. 18 and 19 show the selectivity between HFHIM and HFHNIM. The results show that HFHIM is more selective for transporting urea than creatinine, so with an imprint on the transport percentage results, optimal results are obtained using HFHIM with the best transport.

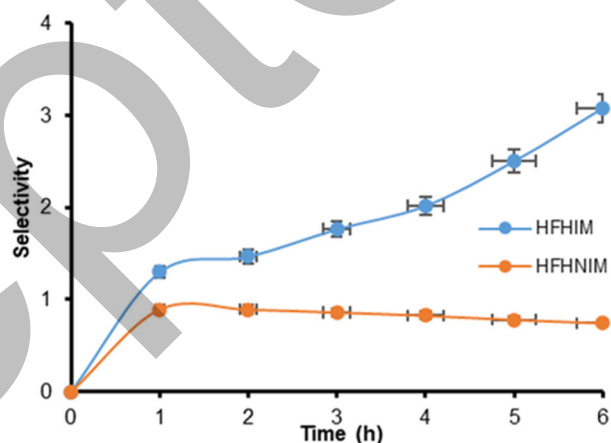


Fig 18. Selectivity of HFHIM and HFHNIM in feed phase

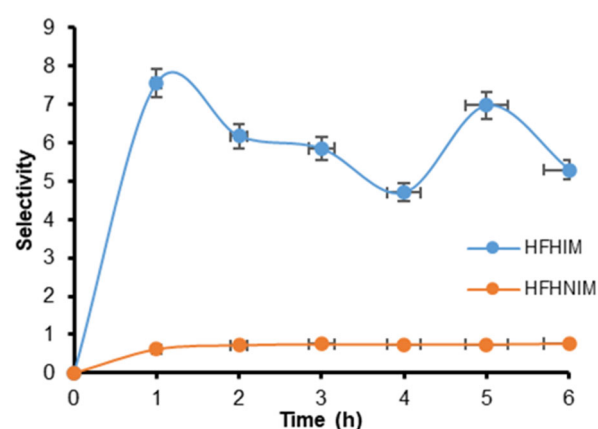


Fig 19. Selectivity of HFHIM and HFHNIM in the receiving phase

This is due to the presence of a printed molecule (template) of urea in the membrane, so that the target



molecule will be more recognizable in transporting urea (the same) compared to creatinine.

#### HFHIM and HFHNIM selectivity for urea vs vitamin B<sub>12</sub>

The membrane selectivity test was carried out by comparing HFHIM and HFHNIM membranes in transporting urea and vitamin B<sub>12</sub> at 50 ppm, which was carried out in separate solutions. HFHIM will be more optimal in transporting urea than HFHNIM. This is due to the presence of a printed molecule (template) of urea in the membrane, so that the target molecule will be better recognized in transporting urea. Fig. 20 and 21 show that HFHIM is more selective for transporting urea than vitamin B<sub>12</sub>, so with an imprint on the transport percentage results, optimal results are obtained using HFHIM with the best transport. This is due to the presence of a printed

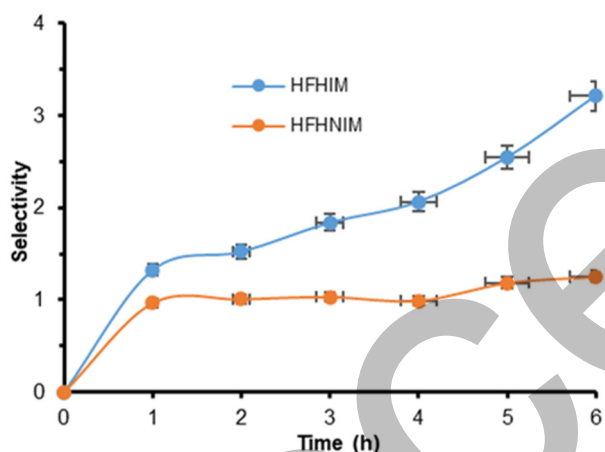


Fig 20. Selectivity of HFHIM and HFHNIM in feed phase

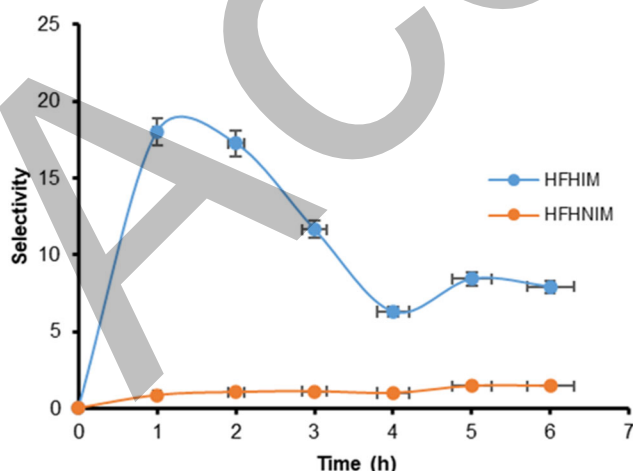


Fig 21. Selectivity of HFHIM and HFHNIM in receiving phase

molecule (template) of urea in the membrane, so that the target molecule will be more recognizable in transporting urea (the same) compared to vitamin B<sub>12</sub> [33]. It can be concluded that HFHIM is said to be selective for urea molecules compared to creatinine and vitamin B<sub>12</sub>, so the order of selectivity is urea > creatinine > vitamin B<sub>12</sub>.

#### CONCLUSION

The transport and selectivity of HFHIM are better than HFHNIM. This is influenced by the template of urea, making the pore size more uniform, stronger, (increased flexibility), and resistance to high temperatures causing hydrophilicity, selectivity, and the performance of the membrane is better, so the order of selectivity is urea > creatinine > vitamin B<sub>12</sub>.

#### ACKNOWLEDGMENTS

The author would like to thank Diponegoro University for the research project, based on the assignment letter of the Directorate of Research and Community Service Deputy for Strengthening Research and Development Ministry of Research and Technology/National Research and Innovation Agency SPK Number: 185-78/UN7.6.1/PP/2022.

#### CONFLICT OF INTEREST

The authors declare that they have no known competing financial interests or personal relationships that could have appeared to influence the work reported in this paper.

#### AUTHOR CONTRIBUTIONS

Conceptualization, methodology, validation, resources, Muhammad Cholid Djunaidi and Yanuardi Raharjo; investigation, Pardoyo; writing—original draft preparation, Nesti Dwi Maharani; review, and editing, Nesti Dwi Maharani and Pardoyo; supervision, Muhammad Cholid Djunaidi, and Yanuardi Raharjo. All authors have read and agreed to the published version of the manuscript.

#### REFERENCES

- [1] Kalantar-Zadeh, K., Jafar, T.H., Nitsch, D., Neuen, B.L., and Perkovic, V., 2021, Chronic kidney disease, *Lancet*, 398 (10302), 786–802.

- [2] Yamada, S., and Inaba, M., 2021, Potassium metabolism and management in patients with CKD, *Nutrients*, 13 (6), 1751.
- [3] Hansen-Estruch, C., Cooper, D.K., and Judd, E., 2022, Physiological aspects of pig kidney xenotransplantation and implications for management following transplant, *Xenotransplantation*, 29 (3), e12743.
- [4] Bays, H.E., Taub, P.R., Epstein, E., Michos, E.D., Ferraro, R.A., Bailey, A.L., Kelli, H.M., Ferdinand, K.C., Echols, M.R., Weintraub, H., Bostrom, J., Johnson, H.M., Hoppe, K.K., Shapiro, M.D., German, C.A., Virani, S.S., Hussain, A., Ballantyne, C.M., Agha, A.M., and Toth, P.P., 2021, Ten things to know about ten cardiovascular disease risk factors, *Am. J. Prev. Cardiol.*, 5, 100149.
- [5] Zaman, S.U., Rafiq, S., Ali, A., Mehdi, M.S., Arshad, A., Rehman, S., Muhammad, N., Irfan, M., Khurram, M.S., Zaman, M.K.U., Hanbazazah, A.S., Lim, H.R., and Show, P.L., 2022, Recent advancement challenges with synthesis of biocompatible hemodialysis membranes, *Chemosphere*, 307, 135626.
- [6] Said, N., Lau, W.J., Ho, Y.C., Lim, S.K., Zainol Abidin, M.N., and Ismail, A.F., 2021, A review of commercial developments and recent laboratory research of dialyzers and membranes for hemodialysis application, *Membranes*, 11 (10), 767.
- [7] Bolton, S., Gair, R., Nilsson, L.G., Matthews, M., Stewart, L., and McCullagh, N., 2021, Clinical assessment of dialysis recovery time and symptom burden: Impact of switching hemodialysis therapy mode, *Patient Relat. Outcome Meas.*, 12, 315–321.
- [8] Yang, H., Liu, H.B., Tang, Z.S., Qiu, Z.D., Zhu, H.X., Song, Z.X., and Jia, A.L., 2021, Synthesis, performance, and application of molecularly imprinted membranes: A review, *J. Environ. Chem. Eng.*, 9 (6), 106352.
- [9] Donato, L., Nasser, I.I., Majdoub, M., and Drioli, E., 2022, Green chemistry and molecularly imprinted membranes, *Membranes*, 12 (5), 472.
- [10] El Hani, O., García-Guzmán, J.J., Palacios-Santander, J.M., Digua, K., Amine, A., and Cubillana-Aguilera, L., 2024, Development of a molecularly imprinted membrane for selective, high-sensitive, and on-site detection of antibiotics in waters and drugs: Application for sulfamethoxazole, *Chemosphere*, 350, 141039.
- [11] Ahmed, J., Rashed, M.A., Faisal, M., Harraz, F.A., Jalalah, M., and Alsareii, S., 2021, Novel SWCNTs-mesoporous silicon nanocomposite as efficient non-enzymatic glucose biosensor, *Appl. Surf. Sci.*, 552, 149477.
- [12] Ahirrao, V., Jadhav, R., More, K., Kale, R., Rane, V., Kilbile, J., Rafeeq, M., and Yeole, R., 2022, An accurate and precise analytical method for estimation of active sulfur trioxide and sulfuric acid in triethylamine sulfur trioxide complex, *Asian J. Pharm. Anal.*, 12 (1), 17–22.
- [13] Raharjo, Y., Ismail, A.F., Othman, M.H.D., Rosid, S.M., Azali, M.A., and Santoso, D., 2021, Effect of polymer loading on membrane properties and uremic toxins removal for hemodialysis application, *J. Membr. Sci. Res.*, 7 (1), 14–19.
- [14] Raharjo, Y., 2020, Polyethersulfone Mixed Matrix Membrane Containing Imprinted Zeolite for Cresol Removal in Hemodialysis Application, *Dissertation*, Universiti Teknologi Malaysia, Malaysia.
- [15] Abdou, A., Elmakssoudi, A., El Amrani, A., JamalEddine, J., and Dakir, M., 2021, Recent advances in chemical reactivity and biological activities of eugenol derivatives, *Med. Chem. Res.*, 30 (5), 1011–1030.
- [16] Djunaidi, M.C., Dwi Maharani, N., Gunawan, G., and Khasanah, M., 2023, Eugenol-based molecular imprinted membrane synthesis as a glucose sensor in honey, *Mater. Today: Proc.*, 80, 1195–1204.
- [17] Djunaidi, M.C., Prasetya, N.B.A., Khoiriyah, A., Pardoyo, P., Haris, A., and Febriola, N.A., 2020, Polysulfone influence on Au selective adsorbent imprinted membrane synthesis with sulfonated polyeugenol as functional polymer, *Membranes*, 10 (12), 390.
- [18] Djunaidi, M.C., Febriola, N.A., and Haris, A., 2021, Molecularly imprinted membrane for transport of urea, creatinine, and vitamin B<sub>12</sub> as a hemodialysis candidate membrane, *Open Chem.*, 19 (1), 806–817.

- [19] Khajavian, M., Vatanpour, V., Castro-Muñoz, R., and Boczkaj, G., 2022, Chitin and derivative chitosan-based structures — Preparation strategies aided by deep eutectic solvents: A review, *Carbohydr. Polym.*, 275, 118702.
- [20] Chen, J., Peng, Q., Peng, X., Zhang, H., and Zeng, H., 2022. Probing and manipulating noncovalent interactions in functional polymeric systems, *Chem. Rev.*, 122 (18), 14594–14678.
- [21] Si, P., and Zhao, B., 2021, Water-based polyurethanes for sustainable advanced manufacture, *Can. J. Chem. Eng.*, 99 (9), 1851–1869.
- [22] Nam, S., and Mooney, D., 2021, Polymeric tissue adhesives, *Chem. Rev.*, 121 (18), 11336–11384.
- [23] Maggay, I.V., Yu, M.L., Wang, D.M., Chiang, C.H., Chang, Y., and Venault, A., 2022, Strategy to prepare skin-free and macrovoid-free polysulfone membranes via the NIPS process, *J. Membr. Sci.*, 655, 120597.
- [24] Ramanuj, V., Sankaran, R., Malenica, L., Cole, K., Day, M., and McCutcheon, J., 2022, Macrovoid resolved simulations of transport through HPRO relevant membrane geometries, *J. Membr. Sci.*, 662, 120958.
- [25] Mamah, S.C., Goh, P.S., Ismail, A.F., Suzaimi, N.D., Yogarathinam, L.T., Raji, Y.O., and El-badawy, T.H., 2021, Recent development in modification of polysulfone membrane for water treatment application, *J. Water Process Eng.*, 40, 101835.
- [26] Arahman, N., Jakfar, J., Dzulhijjah, W.A., Halimah, N., Silmina, S., Aulia, M.P., Fahrina, A., and Bilad, M.R., 2022, Hydrophilic antimicrobial polyethersulfone membrane for removal of turbidity of well-water, *Water*, 14 (22), 3769.
- [27] Azhar, O., Jahan, Z., Sher, F., Niazi, M.B.K., Kakar, S.J., and Shahid, M., 2021, Cellulose acetate-polyvinyl alcohol blend hemodialysis membranes integrated with dialysis performance and high biocompatibility, *Mater. Sci. Eng., C*, 126, 112127.
- [28] Kusworo, T.D., Irvan, I., Kumoro, A.C., Nabilah, Y., Rasendriya, A., Utomo, D.P., and Hasbullah, H., 2022, Advanced method for clean water recovery from batik wastewater via sequential adsorption, ozonation and photocatalytic membrane PVDF-TiO<sub>2</sub>/rGO processes, *J. Environ. Chem. Eng.*, 10 (6), 108708.
- [29] Wang, K.Y., Weber, M., and Chung, T.S., 2022, Polybenzimidazoles (PBIs) and state-of-the-art PBI hollow fiber membranes for water, organic solvent and gas separations: A review, *J. Mater. Chem. A*, 10 (16), 8687–8718.
- [30] Jana, P., Shyam, M., Singh, S., Jayaprakash, V., and Dev, A., 2021, Biodegradable polymers in drug delivery and oral vaccination, *Eur. Polym. J.*, 142, 110155.
- [31] Qamruzzaman, M., Ahmed, F., and Mondal, M.I.H., 2022, An overview on starch-based sustainable hydrogels: Potential applications and aspects, *J. Polym. Environ.*, 30 (1), 19–50.
- [32] Djunaidi, M.C., and Wenten, I.G., 2021, The effect of functional group in polyeugenol for urea, creatinine, and vitamin B<sub>12</sub> transport, *Rasayan J. Chem.*, 14 (2), 1165–1174.
- [33] Djunaidi, M.C., and Wenten, I.G., 2019, Synthesis of eugenol-based selective membrane for hemodialysis, *IOP Conf. Ser.: Mater. Sci. Eng.*, 509 (1), 012069.